RESEARCH PAPER

Green Preparation, Optimization and Antibacterial Activity of Hydroxyapatite Nanoparticles by Using Senna Italica Leaf Extract Against Pathogenic Bacteria Isolated from Postoperative Endophthalmitis

Ali Abbas Jawad 1*, Suzan Saadi Hussain 1, Osama A. Dakhil 2

- ¹ Department of Biology, College of Science, Mustansiriyah University, Baghdad, Iraq
- ² Department of Physics, College of Science, Mustansiriyah University. Baghdad, Iraq

ARTICLE INFO

Article History: Received 10 June 2025

Accepted 25 September 2025 Published 01 October 2025

Keywords:

Antibiotic sensitivity Endophthalmitis Green synthesis HAp-NPs MIC

ABSTRACT

The need to find new antimicrobial compounds and standard testing procedures to control transmissible diseases has increased highly as antibiotic resistance has increased. The Minimum Inhibitory Concentration (MIC) Assay of HAp-NPs nanoparticles was used to measure their antibacterial activity. Without the use of any equipment, MIC can be visually assessed. HAp-NPs nanoparticles exhibited significant antibacterial activity against the isolation of Pseudomonas aeruginosa, Enterobacter cloacae, and Staphylococcus aureus from postoperative endophthalmitis. These bacteria were selected due to their high level of antibiotic resistance and repeatability. An extract from Senna italica leaves was used to create the hydroxyapatite nanoparticles (HAp-NPs) used in this study. The purpose of this study was to investigate the antibacterial properties of environmentally friendly hydroxyapatite nanoparticles (HAp-NPs) against harmful bacteria. Fourier-transform infrared spectroscopy (FTIR), a Field Emission Scanning Electron Microscope (FE-SEM), energy-dispersive X-ray spectroscopy (EDX), and X-ray diffraction analysis (XRD) were used to characterize the synthesized hydroxyapatite powder.

How to cite this article

Dehghankelishadi P, Dorkoosh FA. Green Preparation, Optimization and Antibacterial Activity of Hydroxyapatite Nanoparticles by Using Senna Italica Leaf Extract Against Pathogenic Bacteria Isolated from Postoperative Endophthalmitis. J Nanostruct, 2025; 15(4):2132-2142. DOI: 10.22052/JNS.2025.04.053

INTRODUCTION

The development of nanobiotechnology has produced numerous innovative antibacterial remedies. Nanoparticles are ideal for biological antibacterial activities because of their small size. Nanoparticles have a variety of biological activities, such as antibacterial, antioxidant, anticancer, and radical-scavenging properties, in addition to its abundance of chemically diverse

* Corresponding Author Email: aliabbasbio@uomustansiriyah.edu.iq

organic and inorganic compounds [1]. One of the most challenging and rapidly expanding areas of nanotechnology is the synthesis of nanomaterials. According to [2], nanotechnology in biological sciences holds promise for a wide range of medical applications at the molecular and cellular levels.

Hydroxyapatite (HA) exhibits superior biological qualities and a chemical makeup similar to that of natural bone and teeth. Chemically speaking, apatite is a group of minerals that contain phosphate, while calcium (Ca) apatite is a mineral. HA has the general formula Ca_s(PO₄)₃OH and the unit cell formula $Ca_{10}(PO_4)_6(OH)_2$ [3]. HAp-NPs have antibacterial properties at high concentrations through a variety of mechanisms, such as interactions with proteins and DNA, ion release, mechanical effects on the cell membrane, and the production of reactive oxygen species. They are promising for antibacterial applications in the environment and in medicine because of these mechanisms [4]. The antimicrobial activity increased as the size of the nanoparticles decreased. Certain interactions between nanomaterials and bacterial membrane pores prevent the growth of bacterial populations [5].

With green synthesis, crystal formation can be more precisely controlled. According to [6], nanoparticles (NPs) produced with eco-friendly technologies are inexpensive, flexible, and have a number of potentials uses in the scientific community. Green sources create size- and shape-regulated nanoparticles by stabilizing and reducing agents. plant extracts including sugars, polyphenols, terpenoids, alkaloids, proteins, and

phenolics. The ability of plants to convert inorganic metal ions into nanoparticles has been thoroughly investigated [7].

After cataract surgery, postoperative endophthalmitis is a dangerous side effect. It mostly happens when bacteria, fungi, or microbial flora from the adnexa and surroundings penetrated the globe during surgery. Coagulase-negative staphylococci infections are responsible for the majority of postoperative endophthalmitis cases. Bacillus cereus, Streptococci, Enterococci, and S. aureus are among the gram-positive bacterial species [8]. According to [9], the prevalence of B. cereus in post-traumatic endophthalmitis is ten times higher than that in post-surgical cases. Pseudomonas aeruginosa was the main gramnegative bacterial isolate [10]. Escherichia coli were gram-negative bacteria [11]. Neisseria spp. were Gram-negative cocci, Proteus spp., and Enterobacter spp. The majority of these species exhibit high levels of antibiotic resistance (MDR). The purpose of this study is to ascertain whether synthesis-HAp-NPs has green antibacterial properties against bacteria that have been isolated from the eye and are responsible for postoperative

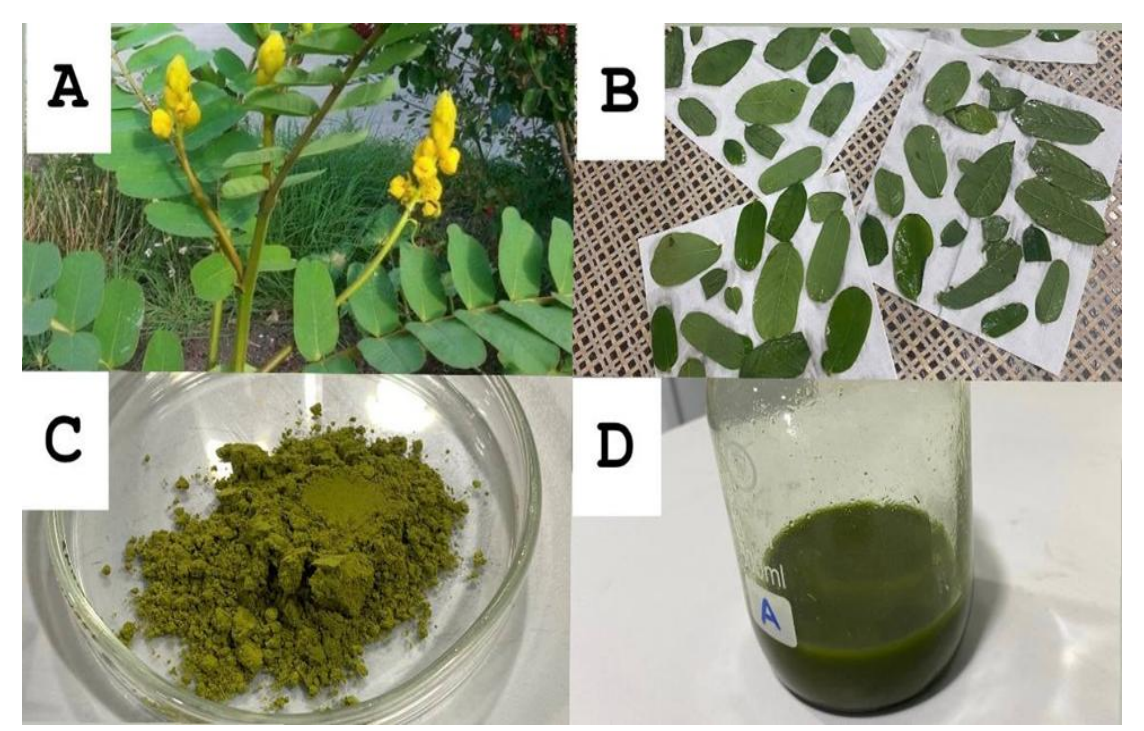


Fig. 1. The steps of preparing Senna italica leaves extract

endophthalmitis.

MATERIALS and METHODS

Plant Material Synthesis

The leaves of Senna italica was collected from my garden, Wash the leaves and dry them, the dried leaves were milled to a fine powder by using lab Powder Grinder, stored in closed containers at room temperature and in the dark until required. 3.0 g of dried leaf powder of Senna italica was macerated separately in 100 mL of 95% ethanol at ambient temperature for two days with occasional shaking and then filtered off. The solvent was evaporated in vacuum to give a crude product. The pH of the extract of Senna leaf was determined using pH Indicator Strips. the pH values of the crude extracts were recorded. As shown in the Fig.

Hydroxyapatite Nanoparticle Synthesis

Without any refining, the following chemicals and substances of analytical grade were used: orthophosphoric acid (H₃PO₄), calcium chloride (CaCl₂), and Sodium hydroxide (NaOH). Ultrapure Milli-Q water was employed. After finding the optimum synthesis parameters, HAp-NPs were synthesized using Senna italica leaf extracts

through the green process as follows. A solution of (0.6 M) orthophosphoric acid (H₂PO₄) was also prepared and combined with the calcium chloride solution. After that, the Senna italica leaf extract was added to the aforementioned mixture and agitated for 1 hour; NaOH was gradually added until the pH reached above 10. After three hours of continuous agitation, a colloidal solution formed from this mixture. The solution was heated in a hot air oven set to 50 °C for 24 hours in order to gradually evaporate the water. The drying process was continued at 50°C for 48 hours to remove the leftover water, resulting in a yellowish, brittle, and porous dry substance. Finally, Grind the material with a mortar and pestle after drying to get rid of the aggregation that formed during the drying process, resulting in ultra-fine HAp- NPs. This method is compatible with [12], But it has been modified and optimal conditions such as temperature, drying and pH have been created to improve the antibacterial effectiveness. As shown in the Fig. 2.

Characterization of HAp-NPs

The properties of NPs determine their potential applications. Hence, different methods and techniques are used for the analysis and

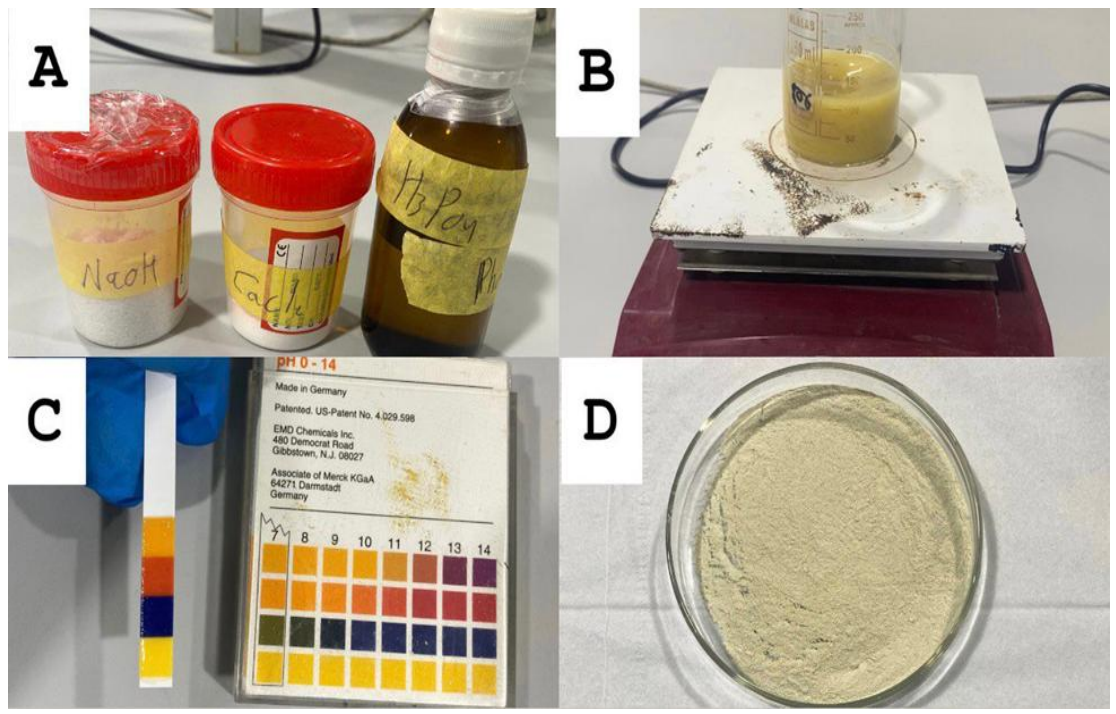


Fig. 2. Explains the steps for preparing the Hydroxyapatite Nanoparticle Synthesis.

characterization of the various physicochemical properties of NPs. I will use the following analyses: Fourier-transform infrared spectroscopy (FTIR), Field Emission Scanning Electron Microscope (FESEM), Energy-dispersive X-ray spectroscopy (EDX), X-ray diffraction analysis (XRD).

Fourier-transform infrared spectroscopy (FTIR)

This method involves exposing a material to infrared light and recording the amount of radiation that is absorbed or transmitted. The resultant spectrum serves as a distinct fingerprint of the sample, from which details about its nature, including the bonds involved, polarity, and oxidation state, can be gleaned [13]. To identify the functional groups in the materials in the 400–4000 cm⁻¹ range, FT-IR analysis was performed using the single reflection ATR method.

Field Emission Scanning Electron Microscope (FE-SEM)

An electron beam is created by an electron gun and directed by a set of lenses to travel vertically through the microscope until it strikes the samples. X-rays and electrons are released from the sample after it is struck by the beam. To produce a three-dimensional image of the sample, detectors are then used to gather the scattered electrons and X-rays (TESCAN, MIRA3, Czechia). SEM gives various details about the NPs, including their size, shape, aggregation, and dispersion [14].

Energy-dispersive X-ray spectroscopy (EDX)

This method depends on exposing the sample to an electron beam. When the electron beam's electrons strike the sample surface, they expel inner-shell electrons. The transition of outer-shell electrons to fill the inner-shell vacancy results in X-rays using a (TESCAN, MIRA3, Czechia). Each element can be used to perform compositional analysis because of its distinct atomic structure, which results in a distinctive X-ray emission pattern [15]. EDX's drawback is that its resulting spectra only provide qualitative compositional information, i.e., the chemical substances present in the sample in an unquantified manner. Nevertheless, peak intensities can provide an estimate of an element's relative abundance in a sample to a certain degree [16]. This method simply involves connecting a small device to an existing SEM or TEM; it does not require complex additional infrastructures. This makes it possible to

use EDX for the simultaneous analysis of chemical composition and SEM or TEM for morphological characterization [17].

X-ray diffraction analysis (XRD)

Measuring the intensities and scattering angles of the X-rays that exit a material after it has been exposed to incident X-rays is the foundation of this technique. For the analysis of NP phase and crystallinity, this method is frequently employed [18]. Using an X-ray diffraction (XRD) instrument (PHILIPS, PW1730, The Netherlands) with Cu radiation at 15406 nm at 35 kV and 30 mA, the phase composition and crystallinity of HA-NPs were examined. Over the 20, data were gathered.

Collection of Pathogenic Specimens

130 samples were collected from hospitals in Baghdad, Iraq, from patients who had postoperative endophthalmitis. Twenty samples had no growth. A total of 25 samples had fungal growth. The 85 samples contained the following kinds of bacteria: Pseudomonas aeruginosa, Escherichia coli, Proteus Spp, Neisseria zoodegmatis, Bacillus cereus, Staphylococcus aureus, Streptococcus pneumoniae, and Enterobacter cloacae. All of these samples were taken using a 30-gauge needle and 0.1-0.2 mL of either aqueous or vitreous humor in aseptic conditions. The culture media utilized were Sabouraud's dextrose agar SDA (incubated at 25°C), chocolate agar CA (incubated at 37°C), and blood agar BA (incubated aerobically at 37°C).

Preparation of bacterial strains

Bacterial strains investigated in the current study were *Staphylococcus aureus*, *Pseudomonas aeruginosa*, and *Enterobacter cloacae*. because of their reproducibility and high resistance to antibiotics. All the bacterial strains were cultured in Mueller-Hinton broth (MHB, Germany) at 37°C for 24 h.

Antibiotic sensitivity studies

The antibiotic susceptibility testing of the aerobic isolates was done by the standard Kirby-Bauer disk-diffusion technique [19]. Antimicrobial susceptibility testing was performed using the modified Kirby-Bauer disk diffusion method on Mueller-Hinton Agar (MHA), following the Clinical and Laboratory Standards Institute (CLSI) guidelines (CLSI M100-Ed35 breakpoints 2025).

J Nanostruct 15(4): 2132-2142, Autumn 2025



Bacteria were classified as multidrug-resistant (MDR) if they exhibited resistance to three or more antibiotic classes.

The antibiotics tested for Gram-positive bacteria included:

 β -lactams: Cefoxitin (FOX 30 μg), Penicillin (P 10 μg). Fluoroquinolones: Levofloxacin (LEV 5 μg), Ciprofloxacin (CIP 5 μg), Ofloxacin (OFX 5 μg).

Aminoglycosides: Gentamicin (CN 10 μ g). Macrolides: Azithromycin (AZM 15 μ g), Chloramphenicol (C 30 μ g), Erythromycin (E 15 μ g). Sulfonamides: Co-trimoxazole (SXT 25 μ g).

Tetracycline: Tetracycline (TE 30 μ g).

Lincosamide: Clindamycin (CD 2 μg).

The antibiotics tested for Gram-negative bacteria included:

 β -lactams: Ceftazidime (CAZ 30 μg), Ticarcillin + clavulanic acid (TIM 85 μg), Piperacillin (PRL 100 μg), Cefepime (FEP 30 μg), Aztreonam (ATM 30 μg).

Fluoroquinolones: Levofloxacin (LEV 5 μ g), Ciprofloxacin (CIP 5 μ g), Ofloxacin (OFX 5 μ g). Aminoglycosides: Gentamicin (CN 10 μ g). Macrolides: Azithromycin (AZM 15 μ g).

Table 1. Shows the sizes of materials and additives in the MIC experiment.

Components	1	2	3	4	5	6	7	8	9	10
B.H.I broth (μl)	100	100	100	100	100	100	100	100	100	100
HAp-NPs stock solution (μl)	10	20	30	40	50	60	70	80	90	100
D.D.W. (μl)	90	80	70	60	50	40	30	20	10	0
Final concentration (mg/ml)	25	50	70	100	125	150	175	200	225	250

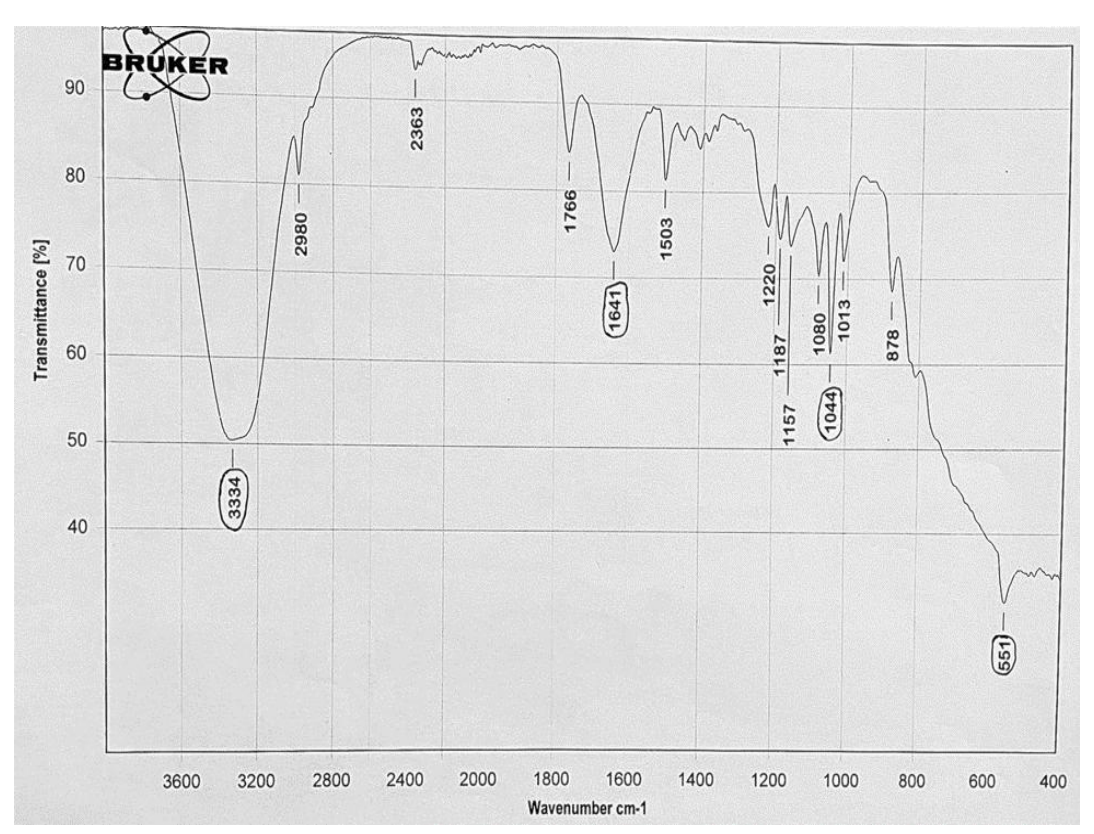


Fig. 3. Chart showing the FT-IR test result.

Carbapenems: Imipenem (IMI 10 μ g), Meropenem (MEM 10 μ g).

Preparation of Resazurin Solution

The resazurin solution was made at 0.02% (wt/vol) according [20]. 10 ml of distilled water were used to dissolve 0.002 grams of resazurin salt powder, which was then vortexed. A Millipore membrane filter (0.2 μm) was used to filter the mixture. For two weeks, the resazurin solution can be stored at 4°C. The study employed resazurin dye as an indicator to measure cell growth. Viable cells' oxidoreductases converted the blue, non-fluorescent resazurin salt to resorufin, changing its color to pink and fluorescent.

Minimum inhibitory concentration (MIC) Assay

There are techniques for analyzing a compound's antimicrobial effects, and the European Committee

on Antimicrobial Susceptibility Testing (EUCAST) and the Clinical Laboratory Standards Institute (CLSI) have approved specific standards. Using the hydroxyapatite nanoparticle stock solution of 500 mg/ml, take quantities in ascending volumes as indicated in the Table 1. diluted distilled water in decreasing amounts to create a final concentration gradient ranging from 25 mg/mL to 250 mg/ml, and then added to the top row of a 96-well plate. Before incubating for 24 hours at 37 °C, 90 µl of Brain Heart Infusion (BHI) broth was added to wells in tubes containing varying concentrations of 10 µl of bacterial suspension with turbidity equal to 0.5 Mc-Farland. as indicated in Table 1. The wells were filled with 0.02% resazurin dye and incubated for an additional 24 hours at 37 °C. Changes in color were noticed. Pink or colorless indicated bacterial growth, whereas blue or purple indicated no bacterial growth. The minimum

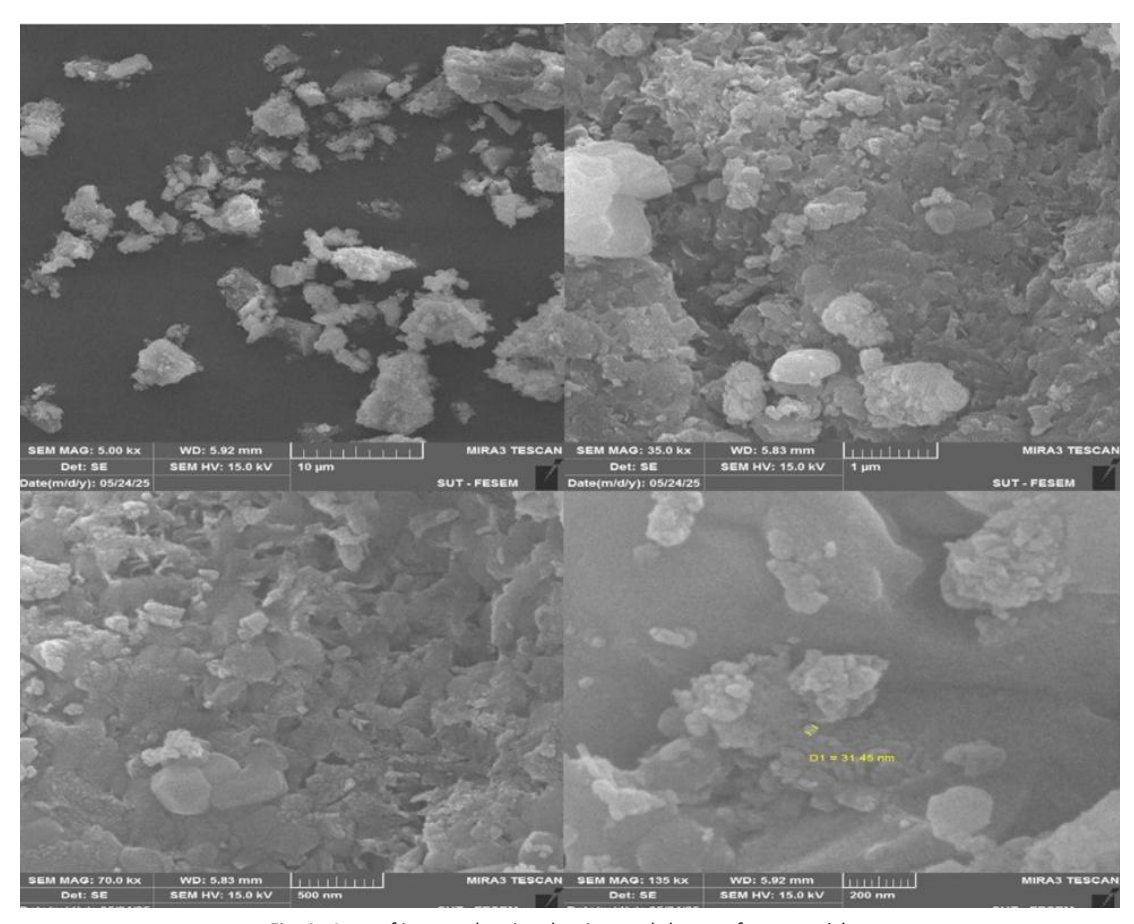


Fig. 4. A set of images showing the sizes and shapes of nanoparticles.

inhibitory concentration of antibacterial agents that prevents bacterial growth (Color remained blue) was used to calculate the MIC value.

RESULTS AND DISCUSSION

Fourier-transform infrared spectroscopy (FTIR)

The FT-IR spectrum of the HAp-NPs is presented in Fig. 3, and it has peaked at 3334, 1641, 1044, and 551 cm⁻¹. The strong peak at 3334 cm⁻¹ corresponds to the characteristic stretching hydroid group. The formation of HAp-NPs is confirmed by absorption peaks at 551 and 1044 cm⁻¹. The absorption peaks at 551 and 1044 cm⁻¹ prove the synthesis of HAp-NPs, and the peaks at 551 cm⁻¹ correspond to the bending vibrations of O-P-O in the phosphate

group PO₄. The presence of the carbonate ion results from the interaction between atmospheric carbon dioxide and the HAp-NPs precursor alkaline solution sample, this reaction has been seen in other studies. The peak located at 1641 cm⁻¹ also corresponds to a CO – group. The results of this investigation are in accordance with those of Zhang and Poinern et al. [21].

Field Emission Scanning Electron Microscope (FE-SEM)

Fig. 4 displays the FE-SEM pictures of the powdered hydroxyapatite that was synthesized. The photos were taken with a magnification of 500x to 10,000x. The pictures make the nanocrystalline

Table 2. Showing the chemical elements, their weights and concentrations.

Element	Apparent Concentration	Wt%	Atomic %	Factory Standard
0	3.82	32.81	49.25	Yes
Р	5.23	17.64	13.67	Yes
Ca	5.12	26.11	15.65	Yes
Cl	1.36	7.44	5.04	Yes
Na	3.29	13.95	14.57	Yes
Al	0.39	2.04	1.82	Yes
Total:		100.00	100.00	

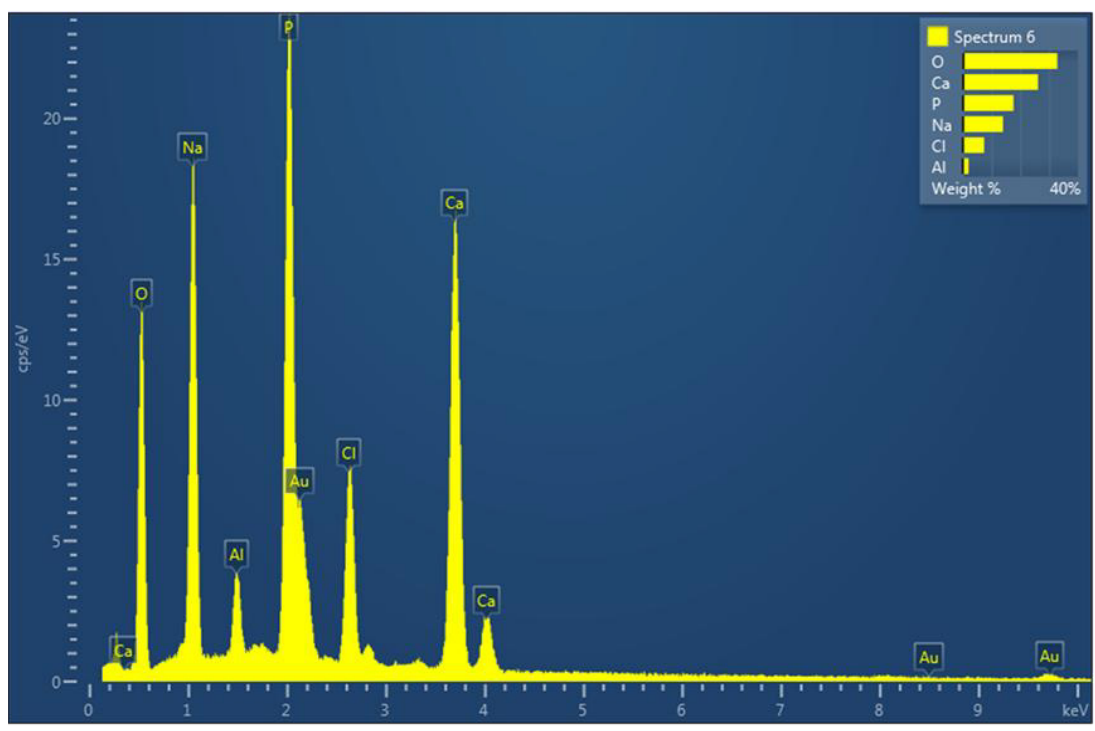


Fig. 5. A diagram showing the chemical composition of a sample.

HA easy to see. Since the generated HA powder is composed of nanocrystalline molecules that form microcrystalline molecules, it has a bulky nature. Agglomerates of irregular shapes were discovered, and they have a propensity to leave pores between them. Pore formations are beneficial because, when utilized as a biomaterial, they allow tissue to

grow on implants inside the body [22].

Energy-dispersive X-ray spectroscopy (EDX)

EDX is semi-quantitative and is affected by sample morphology and equipment calibration. Fig. 5 presents the results of the chemical composition analysis. Ca/P ratios of 1.48 are

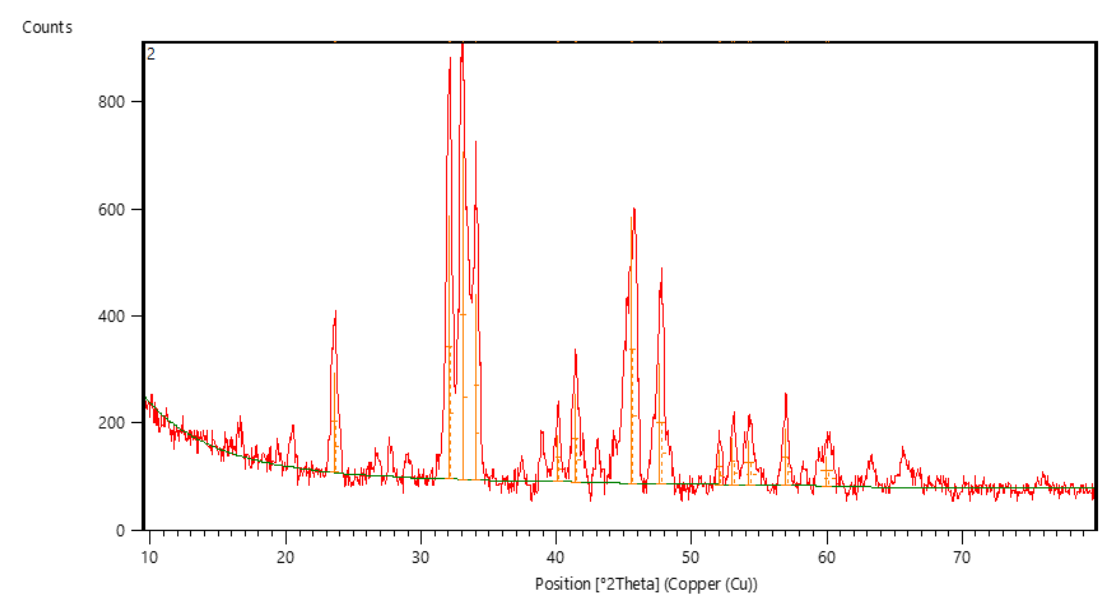


Fig. 6. Chart showing XRD test results.

Table 3. Antibiotic sensitivity (S = Sensitive), (R = Resistance).

		, ,	,, ,		,							
Gram-positive Bacteria	FOX 30 μg	P 10 μg	LEV 5 μg	CIP 5 μg	OFX 5 μg	CN 10 μg	AZM 15 μg	С 30µg	Ε 15 μg	SXT 25 μg	TE 30 μg	CD 2 µg
S. aureus	S	R	S	R	R	R	R	S	R	R	R	R
S. aureus	R	R	R	R	S	R	R	S	S	R	S	R
S. aureus	S	R	R	R	R	R	R	R	R	S	R	R
S. aureus	R	S	R	R	S	R	S	S	R	R	S	R
S. aureus	R	R	R	S	R	R	R	R	S	R	R	R
Gram-negative Bacteria	CAZ 30 μg	TIM 85 μg	PRL 100 μg	FEP 30 μg	ATM 30 μg	LEV 5 μg	CIP 5 μg	OFX 5 μg	CN 10 μg	AZM 15 μg	IMI 10 μg	MEN 10 μg
P.aeruginosa	R	R	S	R	R	R	R	R	R	R	R	R
P.aeruginosa	R	S	R	R	R	S	R	R	R	S	R	R
P.aeruginosa	R	R	R	S	S	S	R	R	R	R	R	R
P.aeruginosa	R	R	S	R	R	R	R	S	R	R	R	S
P.aeruginosa	S	R	S	R	R	S	R	R	R	S	R	R
E.cloacae	R	R	S	R	R	R	R	R	R	S	R	R
E.cloacae	R	R	R	R	S	R	R	R	S	R	R	R
E.cloacae	S	R	R	R	R	S	R	R	R	R	R	S
E.cloacae	R	R	R	R	R	R	R	R	R	S	R	R
E.cloacae	R	R	R	R	R	R	R	R	S	R	R	S

found in the isolated Hydroxyapatite nanoparticles according to the EDX analysis. The average suggests that this percentage is compatible. As wide as 1.47 to 1.88 ratios have been established [23].

X-ray diffraction analysis (XRD)

The XRD pattern of sensitized HAp-NPs powder is shown in Fig. 6. This pattern shows a series of diffraction peaks in the whole spectra of 20 values ranging from 23 to 57° (Fig. 6). The distinct diffraction peaks at 24°, 32°, 33°, 34°, 41.43°, 45.37°,48°, and 57° correspond to miller planes, respectively. This confirms the crystalline structure

of the HAp-NPs produced, and a similar finding was reported by [24].

Antibiotic sensitivity studies

The bacteria showed a high pattern of resistance to antibiotics as shown in the following Table 3.

Minimum Inhibitory Concentration (MIC) Assay

In this study, the application of HAp-NPs as an antimicrobial agent was tested against selected bacteria that cause Endophthalmitis. The results showed that the tested bacteria could be completely inhibited by HAp-NPs. The inhibition of

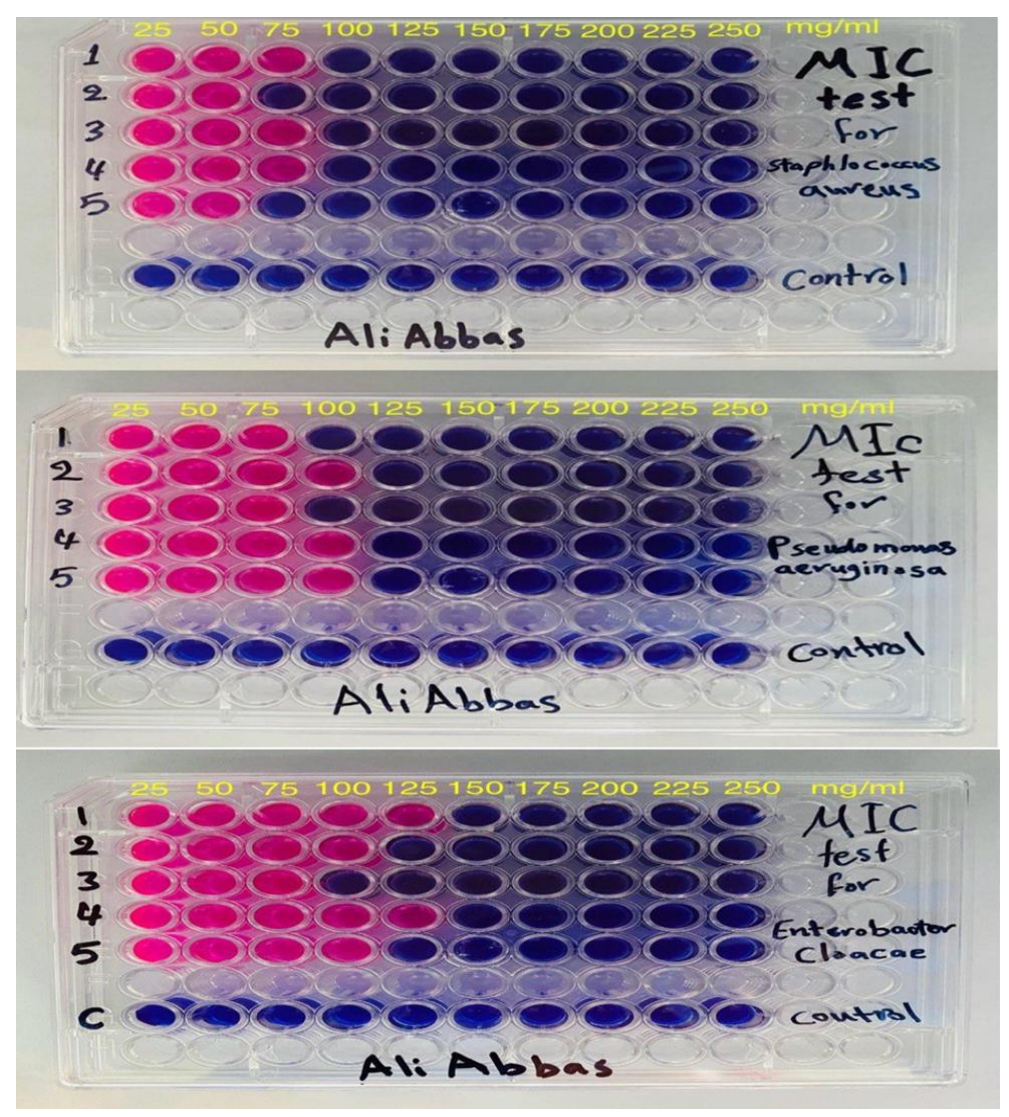


Fig. 7. MIC test for three bacterial types.

bacterial growth was reported to be affected by the concentration of HAp-NPs and the bacteria used in the experiments. The lowest concentration of nanoparticles with no change in color of resazurin was determined as the MIC, is shown in Fig. 7.

The testing material's (HAp-NPs) antibacterial activity was examined against E. cloacae, P. aeruginosa, and S. aureus. The results of the MIC and MBC of the HAp-NPs core shell are compiled in Table 4. Numerous researchers have reported on HAp-NPs' antibacterial activity. The MIC values from earlier research, however, demonstrated a wide range of variation. Since there is no standard technique for determining the antibacterial activity of HAp-NPs and the researchers have used a variety of approaches, it is challenging to compare the results. In this study, Hydroxyapatite particles are effective at killing active bacteria, but only at high concentrations. This is because they are non-toxic, chemically inert, and do not release any active substance into the bacteria. For this reason, they are often modified with antibacterial agents or combined with other nanoproducts to activate them.

Minimum Bactericidal Concentration (MBC)

The MBC was defined as the lowest concentration of the antibacterial agents that completely kill the bacteria. MBC test was performed by plating the suspension from each well of microtiter plates into Mueller Hinton agar (MHA) plate. The plates were incubated at 37°C for 24 h. The lowest concentration with no visible growths on the MHA plate was taken as MBC value. The results of the MIC and MBC of the HAp-NPs core shell are compiled in Table 4.

CONCLUSION

Hydroxyapatite nanoparticles showed significant antibacterial activity against the selected bacteria that causes Endophthalmitis. The findings demonstrate that HAp-NPs may possess antibacterial properties against both bacteria with different efficacies depending on

Table 4. MIC and MBC test result.

No.	Bacterial type	MIC (mg/ml)	MBC(Mg/ml)		
1	S. aureus	100	125		
2	S. aureus	75	100		
3	S. aureus	100	125		
4	S. aureus	100	125		
5	S. aureus	75	125		
6	P. aeruginosa	100	125		
7	P. aeruginosa	125	150		
8	P. aeruginosa	100	100		
9	P. aeruginosa	125	125		
10	P. aeruginosa	125	150		
11	E.cloacae	150	150		
12	E.cloacae	125	125		
13	E.cloacae	100	125		
14	E.cloacae	150	150		
15	E.cloacae	125	125		

concentration and the bacterial strains. Thus, HAp-NPs might be a good alternative to develop as antibacterial agent against the multidrug-resistant strains of bacteria. The applications of HAp-NPs may lead to valuable findings in various fields such as antimicrobial systems.

ACKNOWLEDGEMENTS

The present study is derived from the first author's Master's Thesis and we would like to express our gratitude to all those cooperated in this study.

CONFLICT OF INTEREST

The authors declare that there is no conflict of interests regarding the publication of this manuscript.

REFERENCES

- Arkan JN, Hussain SS, Nawfal HA. Effect of Sulphur Nanoparticles Biosynthesized from Bacillus Coagulans Extract against S. aureus Isolated from Dermatitis Patients in Iraqi Hospitals. Journal of Contemporary Medical Sciences. 2024;10(2).
- Phyto-assisted green synthesis of zinc oxide nanoparticles and its antibacterial and antifungal activity. Research on Crops. 2019;20(4).
- Munir MU, Salman S, Ihsan A, Elsaman T. Synthesis, Characterization, Functionalization and Bio-Applications of Hydroxyapatite Nanomaterials: An Overview. International Journal of Nanomedicine. 2022; Volume 17:1903-1925.
- Silva-Holguín PN, Reyes-López SY. Synthesis of Hydroxyapatite-Ag Composite as Antimicrobial Agent. Dose-Response. 2020;18(3).
- Jaber Sh, Rheima AM, Hussain DH, Al-Marjani MF. Comparing study of CuO synthesized by biological and electrochemical methods for biological activity. Al-Mustansiriyah Journal of Science. 2019;30(1):94-98.
- Lazim KA, Moghaddam HM. Green Synthesis of Nickel Nanoparticles Using Lawsonia inermis Extract and Evaluation of Their Effectiveness against Staphylococcus aureus Al-Mustansiriyah Journal of Science. 2025;36(1):84-91.
- Irwansyah FS, Noviyanti AR, Eddy DR, Risdiana R. Green Template-Mediated Synthesis of Biowaste Nano-Hydroxyapatite: A Systematic Literature Review. Molecules. 2022;27(17):5586.
- 8. Uner OE, Lee D, Horesh R, Jewart B, Seebruck C. Lowering the Incidence of Endophthalmitis Following Intravitreal Anti-VEGF Injection: An Analysis of Aseptic Protocol Adjustment. Ophthalmic Surgery, Lasers and Imaging Retina. 2023;54(9):520-525.
- Kelkar AS, Sharma N, Verma L, Chandorkar SA, Saxena R, Mishra D, et al. Antibiotic prophylaxis for cataract surgery -Practice patterns amongst Indian Ophthalmologists. Indian J Ophthalmol. 2023;71(9):3235-3241.
- 10. Liu Q, Wan L, Zhou J, Huang Y. Ten-Year Analysis of

- Pathogenic Factors and Etiological Characteristics of Endophthalmitis from a Tertiary Eye Center in North China. Infection and Drug Resistance. 2022;Volume 15:3005-3012.
- 11. Joseph J, Sontam B, Guda SJM, Gandhi J, Sharma S, Tyagi M, et al. Trends in microbiological spectrum of endophthalmitis at a single tertiary care ophthalmic hospital in India: a review of 25 years. Eye. 2019;33(7):1090-1095.
- Ganta DD, Hirpaye BY, Raghavanpillai SK, Menber SY. Green Synthesis of Hydroxyapatite Nanoparticles Using Monoon longifolium Leaf Extract for Removal of Fluoride from Aqueous Solution. Journal of Chemistry. 2022;2022:1-13.
- 13. Deepty M, Srinivas C, Kumar ER, Mohan NK, Prajapat CL, Rao TVC, et al. XRD, EDX, FTIR and ESR spectroscopic studies of co-precipitated Mn–substituted Zn–ferrite nanoparticles. Ceram Int. 2019;45(6):8037-8044.
- 14. Vladár AE, Hodoroaba V-D. Characterization of nanoparticles by scanning electron microscopy. Characterization of Nanoparticles: Elsevier; 2020. p. 7-27.
- Groarke R, Vijayaraghavan RK, Powell D, Rennie A, Brabazon D. Powder characterization—methods, standards, and state of the art. Fundamentals of Laser Powder Bed Fusion of Metals: Elsevier; 2021. p. 491-527.
- Nasrollahzadeh M, Atarod M, Sajjadi M, Sajadi SM, Issaabadi
 Plant-Mediated Green Synthesis of Nanostructures: Mechanisms, Characterization, and Applications. Interface Science and Technology: Elsevier; 2019. p. 199-322.
- Giannuzzi LA. Scanning Electron Microscopy and X-Ray Microanalysis 4th Edition, Joseph I. Goldstein, Dale E. Newbury, Joseph R. Michael, Nicholas W.M. Ritchie, John Henry J. Scott, David C. Joy, Springer, 2018, 550 pp. ISBN:978-1-4939-6674-5. Microscopy and Microanalysis. 2018;24(6):768-768.
- Epp J. X-ray diffraction (XRD) techniques for materials characterization. Materials Characterization Using Nondestructive Evaluation (NDE) Methods: Elsevier; 2016. p. 81-124.
- Bauer AW, Kirby WMM, Sherris JC, Turck M. Antibiotic Susceptibility Testing by a Standardized Single Disk Method. Am J Clin Pathol. 1966;45(4_ts):493-496.
- Loo YY, Rukayadi Y, Nor-Khaizura M-A-R, Kuan CH, Chieng BW, Nishibuchi M, et al. In Vitro Antimicrobial Activity of Green Synthesized Silver Nanoparticles Against Selected Gram-negative Foodborne Pathogens. Front Microbiol. 2018;9.
- Poinern GE, Brundavanam, Thi L, Djordjevic, Prokic, Fawcett
 D. Thermal and ultrasonic influence in the formation of
 nanometer scale hydroxyapatite bio-ceramic. International
 Journal of Nanomedicine. 2011:2083.
- Khandelwal H, Prakash S. Synthesis and Characterization of Hydroxyapatite Powder by Eggshell. Journal of Minerals and Materials Characterization and Engineering. 2016;04(02):119-126.
- Mathirat A, Dalavi PA, Prabhu A, G.V YD, Anil S, Senthilkumar K, et al. Remineralizing Potential of Natural Nano-Hydroxyapatite Obtained from Epinephelus chlorostigma in Artificially Induced Early Enamel Lesion: An In Vitro Study. Nanomaterials. 2022;12(22):3993.
- 24. Sonmez E, Cacciatore I, Bakan F, Turkez H, Mohtar YI, Togar B, et al. Toxicity assessment of hydroxyapatite nanoparticles in rat liver cell model in vitro. Human and Experimental Toxicology. 2016;35(10):1073-1083.

J Nanostruct 15(4): 2132-2142, Autumn 2025

